Quantum size effect and persistent hole burning of CuI nanocrystals

Yasuaki Masumoto, Kanae Kawabata,* and Tadashi Kawazoe
Institute of Physics and Center for TARA (Tsukuba Advanced Research Alliance), University of Tsukuba, Tsukuba, Ibaraki 305, Japan
(Received 26 April 1995)

A quantum size effect of nanometer-size CuI microcrystallites (nanocrystals) embedded in glass was investigated and was found to follow the strong-confinement model. Persistent spectral hole burning and thermally annealing hole filling phenomena were observed in samples (CuI nanocrystals in glass). Unusual luminescence behavior (luminescence elongation followed by the increase of light exposure) was also observed. These observed phenomena are explained by the photoionization model of nanocrystals.

Quantum size effects of nanometer-size semiconductor microcrystallites (nanocrystals) have been extensively investigated recently. They are classified into two categories, a strong-confinement regime where electrons and holes are individually quantum confined, and a weak-confinement regime where excitons are quantum confined, depending on the size ratio of R/a_B, where R is the radius of nanocrystals, and a_B the exciton Bohr radius of the bulk crystal.[1–3] Ideally, the strong confinement corresponds to the case of $R/a_B \ll 1$, and the weak confinement to the case of $R/a_B \gg 1$. Strong- and weak-confinement regimes are shown to be two limiting cases of a unified theory for the quantum size effect of nanocrystals given by Kayanuma and quantitative criteria for the boundary between the two regimes are clarified by the theory.[4] The criteria are $R/a_B \geq 4$ for the regime of exciton confinement, $R/a_B \leq 2$ for the regime of individual electron hole confinement, and $2 \leq R/a_B \leq 4$ for the intermediate regime.

CuCl nanocrystals, whose radius is larger than a few nanometers, are the typical materials of the weak confinement,[1,5] because a_B is as small as 0.68 nm. In fact, the experimental blueshift of the exciton structure is well explained by the exciton confinement model, when R ranges from 1.5 to 10 nm. Exciton Bohr radii of CuI is 1.5 nm,[5] which is larger than the Bohr radius of CuCl. If R/a_B is smaller than 4 corresponding to $R \leq 6$ nm, Kayanuma's criteria tell us that CuI nanocrystals do not follow the weak-confinement model.[6] However, the quantum size effect of the CuI nanocrystals has been *a priori* classified into the weak-confinement regime on the experimental data of a sample with unknown size distribution.[5] In another publication,[7] the quantum size effect of the CuI nanocrystals also has been classified into the weak-confinement regime on the experimental data of a few samples with a highly dispersive radius distribution of nanocrystals peaked at 1.6 and 2 nm. The question about the *a priori* assumption and the discrepancy between experiments and theory should be solved by the systematic experimental study of the quantum size effect of CuI nanocrystals.

Another aim of this study is to clarify whether the phenomenon of persistent spectral hole burning (PSHB) occurs in CuI nanocrystals or not. PSHB has been observed in several kinds of semiconductor nanocrystals, such as CdSe, CdSSe, CuCl, and CuBr, embedded in glass or crystals.[8–11] Generality of these phenomena in semiconductor nanocrystals should be tested more by changing the materials. If we can find features related to the PSHB phenomena, they will serve as another hint for the clarification of the phenomena.

Samples studied in this work are nanometer-size CuI nanocrystals embedded in sodium-aluminoborosilicate glass. The size of the nanocrystals was changed by heat treatment and was measured by small-angle x-ray scattering. The small-angle x-ray scattering measurement was done by using a 0.15-nm x-ray, monochromator output of the electron synchrotron orbital radiation, and a position-sensitive proportional counter. For the low-temperature optical measurement, samples were directly

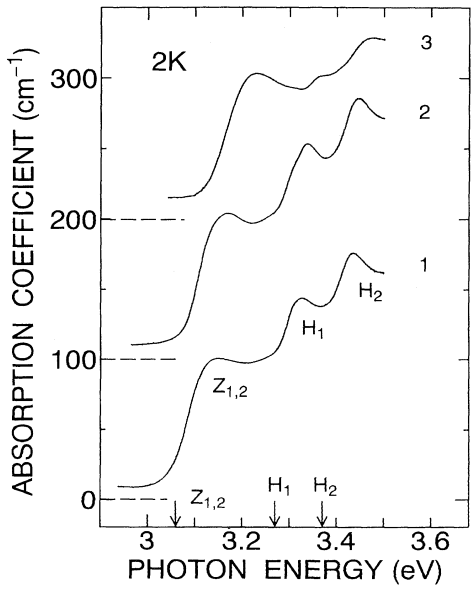

FIG. 1. Absorption spectra of CuI nanocrystals embedded in glass at 2 K. Average radii of nanocrystals 1, 2, and 3 are 4.8, 3.5, and 2.9 nm, respectively. Arrowed positions are $Z_{1,2}$, H_1, and H_2 exciton energies in bulk CuI crystals.

immersed in superfluid He held in a double Pyrex Dewar or were mounted on a cold finger of a closed-cycle-type helium cryostat. The optical absorption measurement was done by using a halogen lamp. The hole burning was done by using a narrow-band dye laser (Lumonics; HD-500) pumped by a Q-switched Nd^{3+}:YAG (yttrium-aluminum garnet) laser (Spectra Physics; GCR-3). The spectral linewidth of the dye laser was 0.014 meV and the pulse duration was 5 ns. A halogen lamp was used for the optical absorption measurement of the sample before and after the narrow-band dye laser irradiation. The absorption spectral change $-\Delta\alpha d$ is defined as the difference in the absorbance of the laser irradiated sample from that of the virgin sample. The luminescence measurement was done by using the third harmonics of the Nd^{3+}:YAG laser.

Absorption spectra of samples show the $Z_{1,2}$ exciton structure whose energy increases with the decrease of the size, as shown in Fig. 1. Besides the $Z_{1,2}$ exciton structure, the H_1 and H_2 exciton structures observed in hexagonal layered CuI (Ref. 12) appear in the nanocrystals of large size but are obscured in smaller size nanocrystals.[7]

Blueshift of the $Z_{1,2}$ exciton structure is plotted in Fig. 3 as a function of the average radius of nanocrystals. The average radius of nanocrystals, R, is estimated from the Guinier plot of the small-angle x-ray scattering data of Fig. 2.[13] The plot shows straight lines, which denote the monodispersive size distribution. The average radius ranges from 2.3 to 5.1 nm. The blueshift calculated on the simplest strong-confinement model is shown by a solid line in Fig. 3. It is expressed by $\Delta E=\hbar^2\pi^2/2\mu R^2$, where $\mu=(1/m_e^*+1/m_h^*)^{-1}$ is the reduced mass.

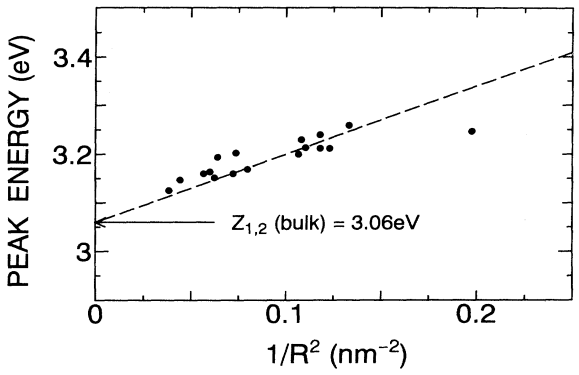

FIG. 3. Peak energy of the $Z_{1,2}$ exciton structure as a function of $1/R^2$, where R is the average radius of nanocrystals. The dashed line shows the calculated blueshift on the strong-confinement model.

Values of $m_e^*=0.33m_0$, $m_h^*=1.40m_0$, and $\mu=0.27m_0$ are adopted for the calculation.[14] The strong-confinement model satisfactorily explains the experimental blueshift. Size-dependent blueshift is much larger than that expected from the weak-confinement model, because exciton translational mass, $1.73m_0$, is 6.4 times larger than the reduced mass. On the basis of the agreement between experimental data and the strong-confinement model, we concluded that the weak-confinement model does not hold, but the strong-confinement model holds for CuI nanocrystals whose ra-

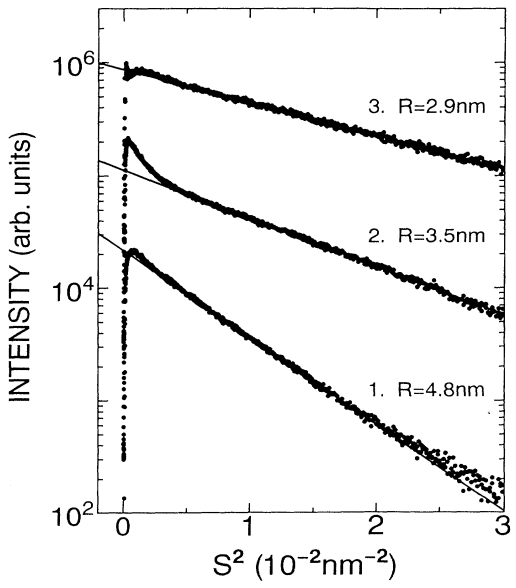

FIG. 2. Guinier plot of the small-angle x-ray scattering intensity. S^2 is defined by $\sin^2\theta/\lambda^2$, where θ is the scattering angle and $\lambda=0.15$ nm is the wavelength of the x ray. Samples 1, 2, and 3, respectively show the absorption spectra 1, 2, and 3 in Fig. 1.

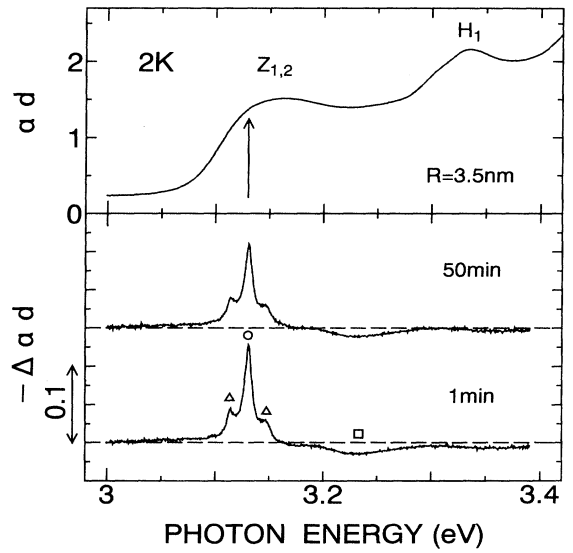

FIG. 4. Top: Absorption spectrum of a virgin sample, CuI nanocrystals embedded in glass. Average radius of nanocrystals is 3.5 nm. Bottom: The absorption spectral change of the sample after the spectrally narrow laser exposure. The sample was excited by 1800 shots of dye laser pulses with the photon energy of 3.130 eV, and an excitation energy density of 80 $\mu J/cm^2$. Long dashed lines show the zero base.

dius ranges from $1.5a_B$ to $3.4a_B$.

Persistent spectral hole burning phenomena were observed in CuI nanocrystals, in the same way as CuCl, CuBr, and CdSe nanocrystals.[8-11] Figure 4 shows the absorption spectrum and the absorption spectral change $-\Delta\alpha d$. The absorption spectral change consists of a spectral hole (open circle), phonon sideband holes (open triangle), and an induced absorption structure (open square). Energy separation between the main hole and the phonon sideband hole agrees with the transverse optical phonon energy of CuI, 16.5 meV.[15] The absorption spectral change is conserved for more than 2 h at 2 K.

The hole depth was found to increase almost in proportion to the logarithm of the laser fluence. Similar logarithmic growth was observed for CuCl and CuBr nanocrystals.[11] The logarithmic hole growth indicates the broad distribution of the burning rate. The broad distribution is explained by the presence of the tunneling process through the potential barrier with broadly distributed barrier height and thickness.[16] Thermally annealing hole filling is also observed. The experimental procedure is the same as described previously.[11] With the increase of annealing temperature, the depth of the hole made at 13.5 K decreases and disappears at about 200 K. The temperature dependence was found to be well fitted by the functional form of

$$\frac{1-\sqrt{kT\ln(\nu_0 t)/V_{\max}}}{1-\sqrt{kT_b\ln(\nu_0 t)/V_{\max}}}$$

for $kT\ln(\nu_0 t) < V_{\max}$, if a fitting parameter $\sqrt{k\ln(\nu_0 t)/V_{\max}}$ is set to be 0.07 $K^{-1/2}$. Here $\ln(\nu_0 t)$ is the logarithm of the product of the frequency factor and the annealing time, which is given by 32–35, and $V_{\max}$ is the maximum barrier height. This functional form is derived on the model for the thermally activated barrier crossing process across the distributed potential height.[17] The maximum barrier height estimated on this model is 0.6 eV.

Photoionization of the site selectively excited nanocrystals and carrier tunneling into traps in the host materials are considered to be the mechanisms for the PSHB phenomenon of CuCl and CuBr nanocrystals.[11] The same scenario is considered to hold for CuI nanocrystals, because characteristic features of hole burning and hole filling observed in CuI nanocrytals are the same as observed in CuCl and CuBr nanocrystals.

The presence of carrier trapping is supported by the following unusual phenomena of luminescence. The luminescence spectrum of CuI nanocrystals shows a Stokes shift from the absorption peak of the $Z_{1,2}$ exciton. The low-energy tail of the luminescence spectrum is below the $Z_{1,2}$ free-exciton energy, 3.06 eV, of bulk CuI. These results suggest the luminescence comes from the localized or bound exciton. With the increase of the in-

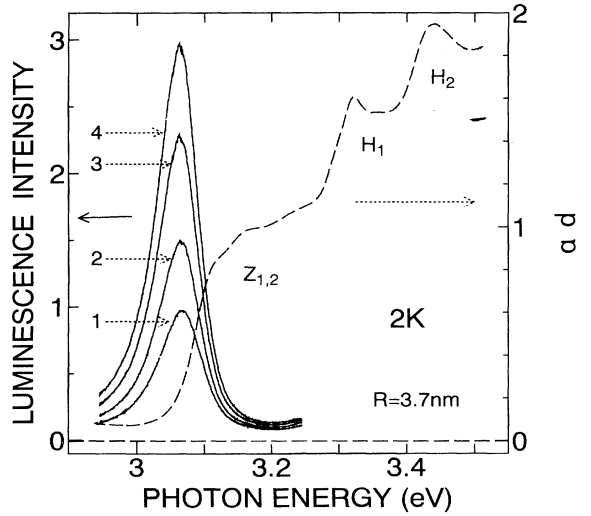

FIG. 5. Luminescence spectra of CuI nanocrystals embedded in glass at 2 K. The absorption spectrum of the sample is shown by a dashed line. The average radius of nanocrystals is 3.7 nm. Excitation laser pulses with the photon energy of 3.49 eV and the excitation density of 5 mJ/cm^2 hit the sample. Spectra 1, 2, 3, and 4 correspond to accumulated luminescence signals of the sample excited by 3000 shots of laser pulses obtained after 0, 4500, 16 500, and 31 500 shots of the laser exposure, respectively.

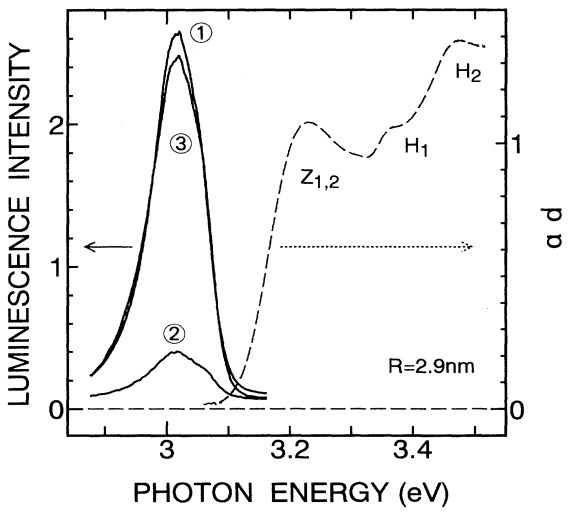

FIG. 6. Thermal cycling effect of the luminescence of CuI nanocrystals embedded in glass. The absorption spectrum of the sample at 2 K is shown by the dashed line. The average radius of nanocrystals is 2.9 nm. Spectrum 1 was taken at 20 K under the excitation density of 50 μJ/cm^2 at 3.49 eV, after the sample had been exposed by integrated excitation density of 600 mJ/cm^2. Then the sample temperature was elevated to 77 K and cooled down to 20 K again. Spectrum 2 was taken just after the temperature cycle at 20 K under the excitation density of 50 μJ/cm^2 at 3.49 eV. After that, the sample was exposed by the integrated excitation density of 600 mJ/cm^2 at 3.49 eV. Spectrum 3 was taken after the 600-mJ/cm^2 exposure at 20 K under the excitation density of 50 μJ/cm^2 at 3.49 eV.

tegrated intensity of laser exposure, the luminescence intensity increases, as is shown in Fig. 5. However, the luminescence intensity is quenched after the annealing cycle, as is shown in Fig. 6. These characteristic phenomena of luminescence are explained, if the carrier trapping at the capture centers in the host glass is saturated with the increase of the laser fluence and if trapped carriers are released with the rise in temperature. We speculate localized or bound excitons formed from free excitons in nanocrystals are radiatively annihilated or nonradiatively decay through ionization, tunneling, and capture by traps in the host glass. The number of traps that are easily accessible by tunneling from nanocrystals are finite and traps seized by carriers become ineffective. This is the reason that the carrier trapping at the capture centers is saturated. A rise in temperature causes the thermal activation of the trapped carriers at the capture centers. Activated carriers are radiatively or nonradiatively annihilated. As a result, traps in the host become effective again. In this way, the above-mentioned unusual phenomena of luminescence are explained by the same scenario as is used to explain the PSHB phenomena.

In summary, the quantum size effect of nanometer-size CuI microcrystallites (nanocrystals) was investigated. Size-dependent blueshift of the $Z_{1,2}$ exciton structure was well explained by the strong-confinement model. Persistent spectral hole burning and thermally annealing hole-filling phenomena were observed. The characteristics of the observed phenomena are the same as observed in CuCl and CuBr nanocrystals. Photoionization of nanocrystals and carrier tunneling into traps in the host glass are considered to be the mechanism for the PSHB phenomena. Unusual luminescence behavior (luminescence elongation with the increase of the light exposure) was observed. This observation is consistent with the photoionization model of nanocrystals.

Small-angle x-ray scattering experiments were done at the Photon Factory (PF) of the National Laboratory for High Energy Physics by the approval of the PF Advisory Committee (Proposals 92-117). The authors wish to thank Professor Y. Amemiya in PF for his guidance to the small-angle x-ray scattering experiments. This work was supported in part by TARA (Tsukuba Advanced Research Alliance) project in University of Tsukuba.

---

*Present address: R&D Laboratories for Photographic Materials, KONICA Corp., Hino, Tokyo 191, Japan.

[1]A. I. Ekimov, Al. L. Efros, and A.A. Onushchenko, Solid State Commun. **56**, 921 (1985).

[2]L. Brus, IEEE J. Quantum Electron. **QE-22**, 1909 (1986).

[3]A. D. Yoffe, Adv. Phys. **42**, 173 (1993).

[4]Y. Kayanuma, Phys. Rev. B **38**, 9797 (1988).

[5]T. Itoh, Y. Iwabuchi, and T. Kirihara, Phys. Status Solidi B **146**, 531 (1988).

[6]As for CuBr, exciton Bohr radius is 1.25 nm. The weak confinement model does not hold for CuBr nanocrystals, but a donorlike exciton model explains the experimental data of them, when R/a_B ranges from 1 to 3. Because of rather large hole mass, hole localization at the center of nanocrystals takes place. See A. I. Ekimov, Al. L. Efros, M. G. Ivanov, A. A. Onushchenko, and S. K. Shumilov, Solid State Commun. **69**, 565 (1989).

[7]O. Gogolin, Yu. Berosashvili, G. Mschvelidze, E. Tsitsishvili, S. Oktjabrski, H. Giessen, A. Uhrig, and C. Klingshirn, Semicond. Sci. Technol. **6**, 401 (1991).

[8]Y. Masumoto, L. G. Zimin, K. Naoe, S. Okamoto, and T. Arai, Mater. Sci. Eng. B **27**, L5 (1994).

[9]K. Naoe, L. G. Zimin, and Y. Masumoto, Phys. Rev. B **50**, 18 200 (1994).

[10]Y. Masumoto, Jpn. J. Appl. Phys. **34**, Suppl. 34-1, 8 (1995).

[11]Y. Masumoto, S. Okamoto, T. Yamamoto, and T. Kawazoe, Phys. Status Solidi B **188**, 209 (1995).

[12]M. Cardona, Phys. Rev. **129**, 69 (1963).

[13]A. Guinier and G. Fournet, *Small-Angle Scattering of X-Rays* (Wiley, New York, 1955).

[14]C. I. Yu, T. Goto, and M. Ueta, J. Phys. Soc. Jpn. **34**, 693 (1973).

[15]*Physics of II-VI and I-VII Compounds, Semimagnetic Semiconductors,* edited by O. Madelung, Landolt-Börnstein, New Series, Group III, Vol. 17, Pt. b (Springer-Verlag, Berlin, 1982).

[16]R. Jankowiak, R. Richert, and H. Bässler, J. Phys. Chem. **89**, 4569 (1985).

[17]W. Köhler, J. Meiler, and J. Friedrich, Phys. Rev. B **35**, 4031 (1987).